

## An *in situ* study of the effects of surface anisotropy on the remote sensing of burned savannah

S. N. TRIGG\*†, D. P. ROY†‡ and S. P. FLASSE§

†Department of Geography, 2181 LeFrak Hall, University of Maryland, College Park, Maryland 20740, USA

‡NASA Goddard Space Flight Center, Code 614.5, Greenbelt, Maryland 20771, USA

§Flasse Consulting, 3 Sycamore Crescent, Maidstone, Kent ME16 0AG, England, UK

(Received 22 November 2004; in final form 18 January 2005)

This Letter presents field-based evidence of the perturbing effects of surface anisotropy on the remote sensing of burned savannah. The analysis is based on bidirectional spectral reflectance data collected at different solar illumination angles and convolved to Moderate-resolution Imaging Spectroradiometer (MODIS) reflective bands. Results from a grass savannah site show that burning reduces the anisotropy of the surface compared to its pre-burn state. In contrast, at a shrub savannah site, burning reduces or increases surface anisotropy. Spectral indices defined from 1.240  $\mu\text{m}$  and 2.130  $\mu\text{m}$  reflectance, and 1.640  $\mu\text{m}$  and 2.130  $\mu\text{m}$  reflectance, provided stronger diurnal separation between burned and unburned areas than individual reflectance bands but do not eliminate anisotropic effects. The Normalized Difference Vegetation Index (NDVI) provides weak diurnal separation relative to these near- and mid-infrared based indices. Implications of the findings are discussed for burned area mapping.

### 1. Introduction

Satellite remote sensing provides the only means to monitor vegetation burning at regional to global scales. Detecting burned areas remotely requires an understanding of which spectral bands are sensitive to changes caused at the surface by burning. It also requires knowledge of how measurements made in these bands are affected by exogenous factors, hereafter referred to as perturbing factors (Pinty and Verstraete 1992, Trigg and Flasse 2001). Perturbing factors include variation in pre-burn surface conditions, such as the photosynthetic state and type of vegetation, and variation in atmospheric constituents above the burned surface, such as water vapour and smoke aerosols (Miura *et al.* 1998, Pereira 2003).

A less explicitly acknowledged perturbing factor, at least in burned area detection studies, is the effect of surface anisotropy. Most land surfaces are strongly anisotropic at optical wavelengths, that is, they reflect different amounts of light depending on the angles at which they are illuminated and viewed (Kimes 1983). Surface anisotropy is therefore a perturbing factor that may complicate the detection of burned areas using wide field of view and multi-temporal satellite data (Roy *et al.* 2002, Stroppiana *et al.* 2002). Understanding the impact of anisotropy on remote sensing applications can be informed by examining *in situ* spectral data

---

\*Corresponding author. Email: [trigg@umd.edu](mailto:trigg@umd.edu)

collected on surfaces of interest at different angles of observation and illumination (Sandmeier 2000). However, although multi-angle data have been provided for numerous studies of vegetation, and of a burned surface created in a laboratory (Lajas 2000), a review of relevant literature revealed no field-based measurements that capture the anisotropy of burned areas or study how this may affect burned area detection.

This Letter provides *in situ* evidence of the anisotropy of burned areas using reflectance data measured using a spectroradiometer over nine hours at burned and unburned shrub and grass sites in Namibia. Using these data converted to Moderate-resolution Imaging Spectroradiometer (MODIS) bands the Letter assesses if burning alters the anisotropy of the post-burn surface relative to its pre-burn condition, and whether the spectral contrast between burned and unburned vegetation varies with solar angle. The Letter also explores the effects of anisotropy on commonly used spectral indices.

## 2. Materials and methods

### 2.1 Reflectance measurement

Diurnal spectral reflectance measurements were made at a shrub site and a grass site in Namibia (17.85646° S, 23.42280° E). All measurements were made in the July burning season. Measurements were made at two locations at the shrub site (unburned shrub and adjacent burned shrub) and at two locations at the grass site (unburned grass and adjacent burned grass). At each of the four locations, a single spectrum was measured every hour between 10 a.m. and 6 p.m. GMT. In this way, nine spectra were measured at each of the four locations (i.e. a total of 36 independently measured spectra). The local solar zenith and azimuth angles at the time of these measurements are illustrated in figure 1.

All spectra were collected using a GER3700 spectroradiometer pointing vertically at the surface from 1.6 m above the ground and using a Spectralon reference panel (Trigg and Flasse 2000).

The underlying highly reflective Kalahari sand was revealed partially after burning and was overlain with a heterogeneous cover of low reflectance char. The four locations are illustrated in figure 2 with the spectroradiometer field of view superimposed.

The grass site (figure 2(a) and (b)) comprised senescent 0.4 m high *Eragrostis pallens* that burned almost completely, whereas the shrub site (figure 2(c) and (d)) comprised wilted but still green 0.5 m high *Diospyros chamaethamnus* that burned to reveal woody stems. Shadows cast by the unburned and burned elements were most evident in the shrub site.

### 2.2 Post processing

The 36 spectra were each convolved to the seven MODIS reflectance wavebands using MODIS filter functions (Trigg and Flasse 2000). Measurements and results for the two shortest wavelength MODIS bands, blue (0.4690  $\mu\text{m}$ ) and green (0.555  $\mu\text{m}$ ), are not described here as they do not discriminate strongly between burned and unburned surfaces (Trigg and Flasse 2000, 2001, Roy *et al.* 2002). The reflectance measurement viewing geometry was fixed while the solar geometry (azimuth and zenith) was calculated from the date, time and location of measurement and using a standard astronomical model (Standish *et al.* 1992).

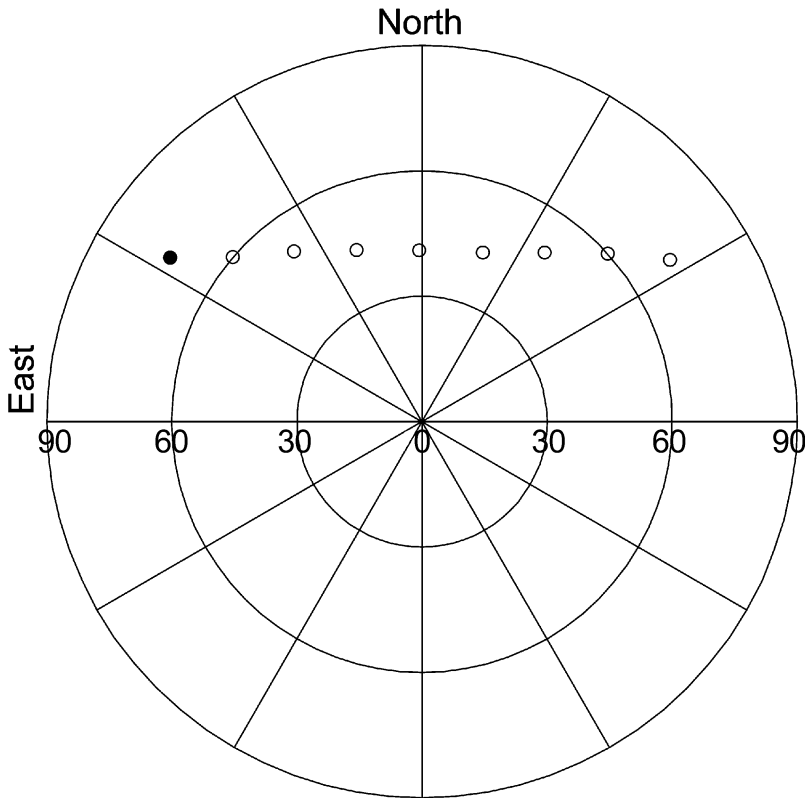


Figure 1. Polar plot illustrating the local solar zenith and azimuth angles for nine spectroradiometer measurements (circles) made hourly from 10 a.m. (solid circle) to 6 p.m. GMT. The straight lines show solar azimuth and the curves show solar zenith spaced every 30°.

To investigate anisotropic effects on spectral indices used for mapping burned areas, three indices, the Normalized Difference Vegetation Index (NDVI), VI57 and VI67, were computed using the following ‘normalized’ formulation:

$$\text{Index} = \frac{(\rho_j - \rho_i)}{(\rho_j + \rho_i)} \quad (1)$$

where  $\rho$ =MODIS band reflectance, and for NDVI,  $i$ =band 1 (0.645  $\mu\text{m}$ ),  $j$ =band 2 (0.858  $\mu\text{m}$ ); VI57,  $i$ =band 7 (2.130  $\mu\text{m}$ ),  $j$ =band 5 (1.240  $\mu\text{m}$ ); VI67,  $i$ =band 7 (2.130  $\mu\text{m}$ ),  $j$ =band 6 (1.640  $\mu\text{m}$ ).

The NDVI was chosen because it has been used often for burned area detection, particularly in boreal regions (Kasischke and French 1995). VI57 and VI67 were chosen because they are defined in MODIS bispectral spaces that discriminate strongly between burned and unburned vegetation (Trigg and Flasse 2001, Roy and Landmann 2005).

### 2.3 Measures to quantify anisotropy and separability

The anisotropy of the reflectance and index measurements was quantified for each location as the difference between the maximum and minimum values observed over

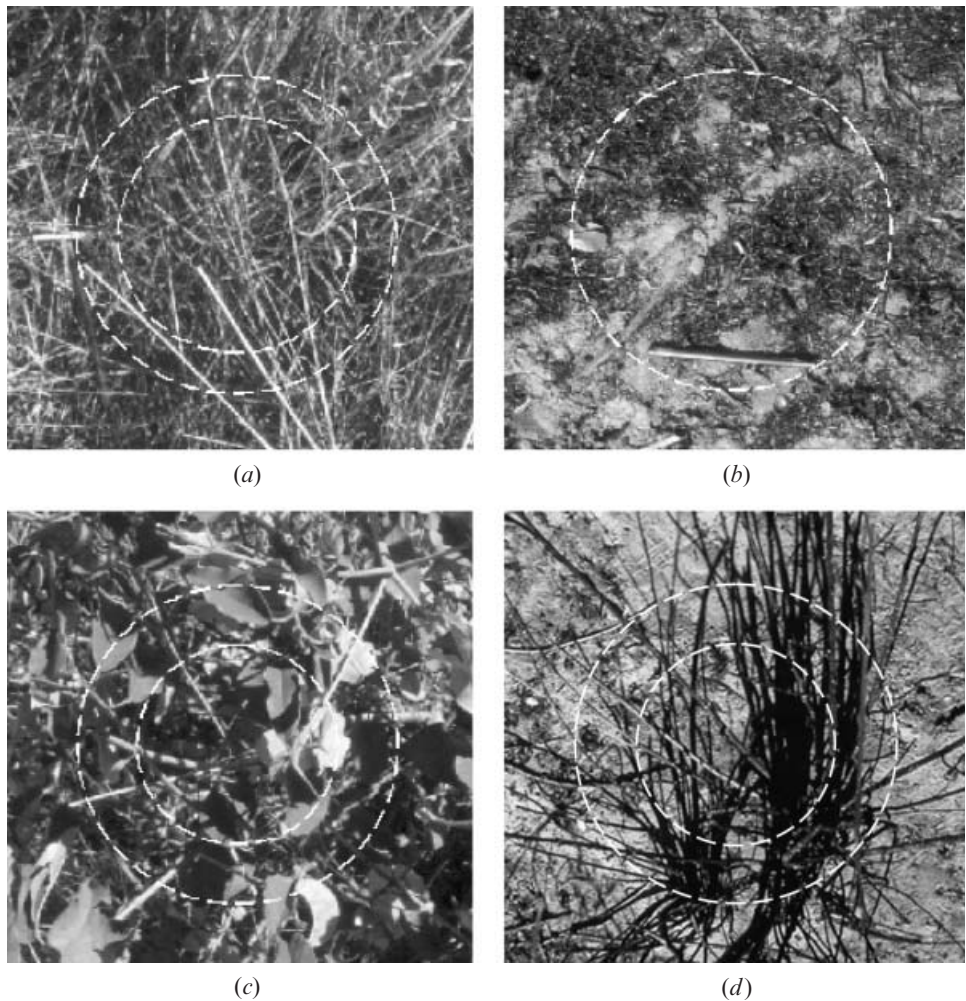


Figure 2. Photographs of the unburned (left column) and burned (right column) grass (*a* and *b*) and shrub (*c* and *d*) sites. The outer circle shows the spectroradiometer surface field of view (28 cm diameter) and the inner circle shows the field of view at the canopy top.

the nine-hour period, i.e. the range ( $R$ ). A zero  $R$  value indicates a Lambertian surface; for all other surfaces,  $R$  will increase with anisotropy. This simple measure allows comparison of how the different band and index values at each site are affected by the anisotropy of the surface, including whether burning alters the anisotropy of each post-burn surface relative to its pre-burn condition. Alternative measures, based on the variation about a fixed or mean value, were not used because of their sensitivity to near-zero values.

Bands or indices used to detect burned areas should provide both a distinct separation of burned and unburned values and insensitivity to perturbing factors (Verstrate and Pinty 1996). Accordingly, a separability measure was used to quantify the ability of the reflectance and index measurements to discriminate between burned and unburned vegetation in conditions of varying solar

illumination. The  $M$  statistic (Swain and Davis 1978) was used:

$$M = (\mu_u - \mu_b) / (\sigma_u + \sigma_b) \quad (2)$$

where  $\mu_u$  and  $\sigma_u$  are the mean and the standard deviation of the nine-hourly unburned values and  $\mu_b$  and  $\sigma_b$  are the mean and the standard deviation of the nine-hourly burned values. Higher  $M$  values imply greater diurnal burned–unburned discrimination.

### 3. Results

#### 3.1 *The effect of burning on surface anisotropy*

Figure 3 illustrates the reflectance and spectral index values for the unburned (open circles) and burned (closed circles) grass (*a*) and shrub (*b*) sites. These data are plotted against the product of the solar zenith and the sine of the solar azimuth as figure 1. The plots also show  $R$  values used to quantify anisotropy.

In figure 3, burning reduces reflectance in all bands, except band 7, which has been observed previously (e.g. Roy *et al.* 2002, Trigg 2002). In each band, reflectance exhibits anisotropy, i.e. it varies with solar illumination geometry associated with different proportions of shadowed vegetation and ground being viewed. Except for band 7 shrub, the unburned surfaces are more anisotropic (higher  $R$ ) than their burned equivalents. In all bands, the burned grass reflectance is only weakly anisotropic, whereas the burned shrub reflectance is considerably more anisotropic. For example, for any band, the burned shrub  $R$  values are more than four times the burned grass  $R$  values. The relatively strong anisotropy of the burned shrub is due to the presence and vertical structure of the unburned stems and their shadows (figure 2).

The different scaling for reflectance and index values precludes comparison of their  $R$  values. The results shown in figure 3 for NDVI, VI57 and VI67, indicate that spectral indices may reduce but not eliminate anisotropic effects (Gao *et al.* 2002). Except for VI67 shrub, the unburned index values show higher  $R$  values than their burned equivalents.

#### 3.2 *Surface anisotropy as a perturbing factor on burned–unburned discrimination*

Figure 4 illustrates the diurnal burned–unburned separability,  $M$ , of the reflectance bands and spectral indices for the grass and shrub sites.

All the reflectance bands show greater diurnal burned–unburned discrimination for grass rather than shrub. This is because the burned grass is only weakly anisotropic compared to the burned shrub. The strongest reflectance discrimination is achieved in the near-infrared bands (2 and 5) and the weakest in the mid-infrared band (7). The mid-infrared band 6 provides strong discrimination at the grass site but the weakest discrimination of any band at the shrub site, which has been observed previously for at-nadir measurements made at this site (Trigg 2002).

The VI57 and VI67 exhibit higher  $M$  values (i.e. increased diurnal burned–unburned discrimination) relative to the reflective bands (figure 4). This is because for these indices the differences between the mean unburned and burned values are generally larger than the anisotropy in the unburned and burned values (figure 3). NDVI provides low separation (low  $M$  values) for these data because of the small difference between pre- and post-burn mean NDVI.

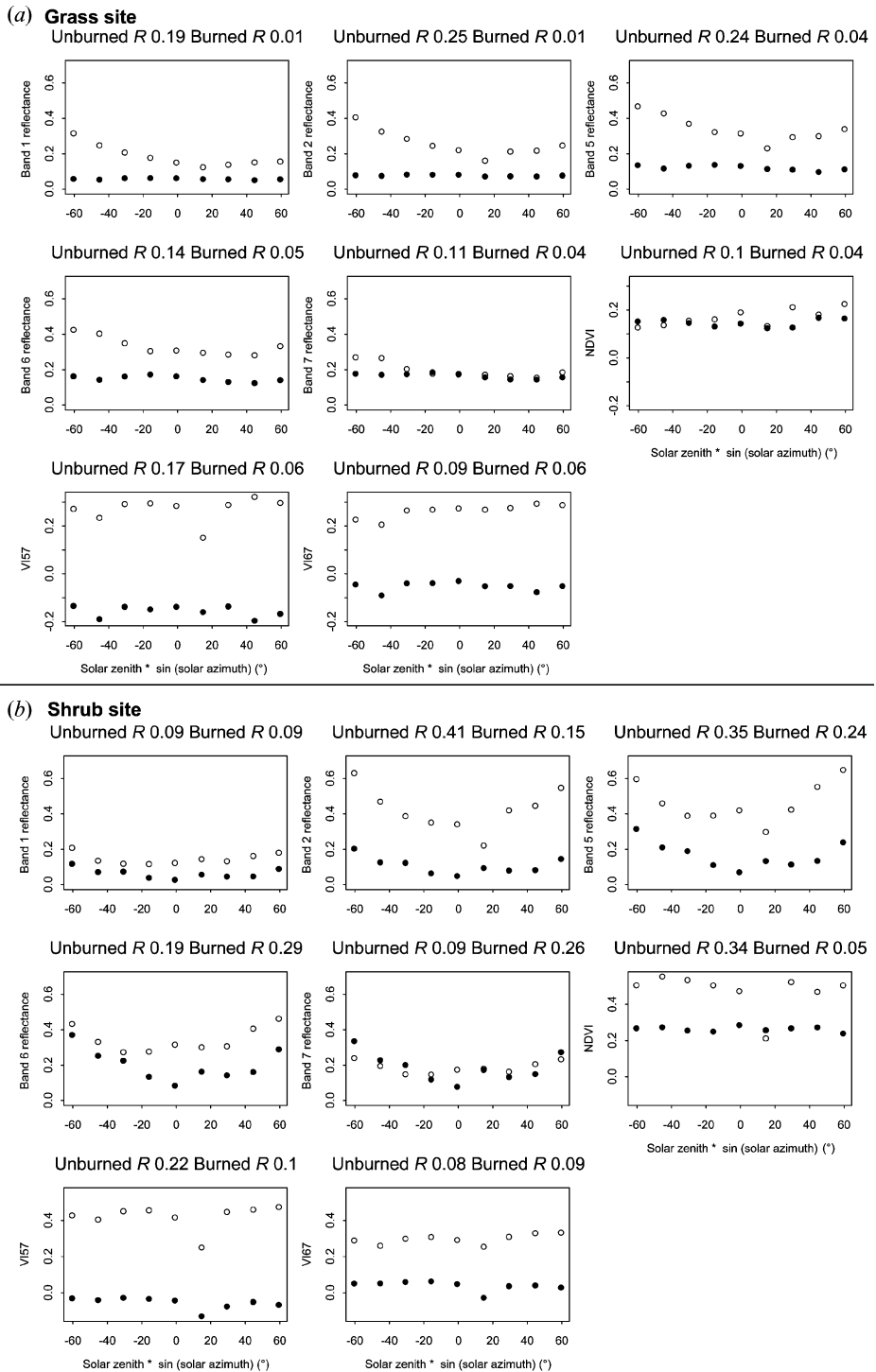


Figure 3. Spectroradiometer reflectance and spectral index values for the unburned (open circles) and burned (closed circles) grass (a) and shrub (b) sites. Reflectance measurements are illustrated for MODIS bands 1 ( $0.645 \mu\text{m}$ ), 2 ( $0.858 \mu\text{m}$ ), 5 ( $1.240 \mu\text{m}$ ), 6 ( $1.640 \mu\text{m}$ ) and 7 ( $2.130 \mu\text{m}$ ). The  $R$  anisotropy measure is shown for the unburned and burned data.

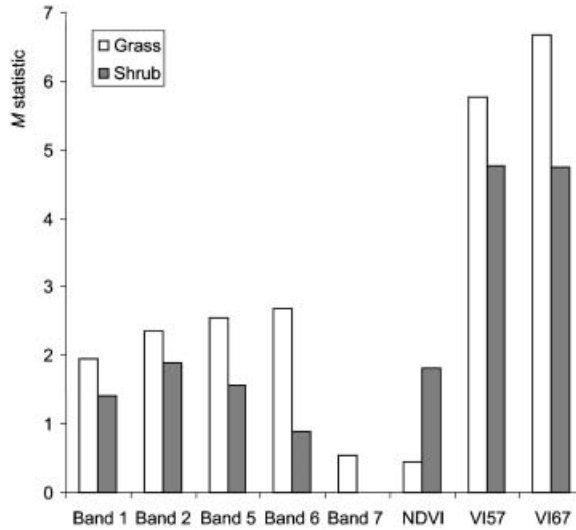


Figure 4. Diurnal burned–unburned separability,  $M$ , of the reflectance bands and spectral indices for the grass and shrub sites.

#### 4. Conclusion

Although these findings are limited to small sites, they add field-based evidence of how varying solar angle coupled with surface anisotropy perturb the spectral separation of burned and unburned vegetation at reflective wavelengths.

Findings demonstrate that the anisotropy of a burned surface is affected by its three-dimensional structure. Fire at a grass savannah site burned most material to leave a flat surface with low reflectance anisotropy, whereas fire at a shrub site left a more structured configuration of charred stems and shadows with greater anisotropy. One implication of this finding for further analysis is that the anisotropy of shrub would have been reduced further post-burn had the fire consumed the stems rather than merely charring them. The anisotropy of burned vegetation may be expected to vary with factors that affect completeness of combustion, such as fire intensity and the associated timing of burning within the fire season.

The analysis provides evidence that, in the absence of a model of the directional dependence of reflectance on the Sun–target–sensing geometry (Roy *et al.* 2002), individual reflectance bands may provide a poor basis for the automated detection of burned areas using wide field of view data, such as MODIS, and/or using multi-temporal satellite data when the solar geometry changes, for example, Landsat time series. Normalized indices defined from 1.240  $\mu\text{m}$  and 2.130  $\mu\text{m}$  reflectance, and 1.640  $\mu\text{m}$  and 2.130  $\mu\text{m}$  reflectance, provide stronger diurnal separation between burned and unburned areas than individual reflectance bands and generally reduce but do not eliminate anisotropic effects. Conversely, NDVI provides low separation (low  $M$  values) for these data because of the small difference between pre- and post-burn mean NDVI. These findings confirm that the optimal threshold needed to discern burned from unburned areas may vary with the geometry of illumination and observation. This may help explain why burned area mapping routines that ignore angular effects often prove difficult to automate over large areas.

**References**

- GAO, F., JIN, Y., LI, X., SCHAAF, C.B. and STRAHLER, A.H., 2002, Bidirectional NDVI and atmospherically resistant BRDF inversion for vegetation canopy. *IEEE Transactions on Geoscience and Remote Sensing*, **40**, pp. 1269–1278.
- KASISCHKE, E.S. and FRENCH, N.H.F., 1995, Locating and estimating the aerial extent of wildfires in Alaskan boreal forests using multiple-season AVHRR NDVI composite data. *Remote Sensing of Environment*, **51**, pp. 263–275.
- KIMES, D.S., 1983, Dynamics of directional reflectance factor distributions for vegetation canopies. *Applied Optics*, **22**, pp. 1364–1372.
- LAJAS, D., 2000, Documenting the bidirectional reflectance: model and measurements. MSc thesis, Space Applications Institute–JRC and University of Lisbon.
- MIURA, T., HUETE, A.R., VAN LEEUWEN, W.J.D. and DIDAN, K., 1998, Vegetation detection through smoke filled AVIRIS images: an assessment using MODIS band passes. *Journal of Geophysical Research*, **103**, pp. 32 001–32 011.
- PEREIRA, J.M.C., 2003, Remote sensing of burned areas in tropical savannas. *International Journal of Wildland Fire*, **12**, pp. 259–270.
- PINTY, B. and VERSTRAETE, M., 1992, On the design and validation of bidirectional reflectance and albedo models. *Remote Sensing of Environment*, **41**, pp. 155–167.
- ROY, D. and LANDMANN, T., 2005, Characterizing the surface heterogeneity of fire effects using multi-temporal reflective wavelength data. *International Journal of Remote Sensing*, **26**, pp. 4197–4218.
- ROY, D.P., LEWIS, P.E. and JUSTICE, C.O., 2002, Burned area mapping using multi-temporal moderate spatial resolution data—a bi-directional reflectance model-based expectation approach. *Remote Sensing of Environment*, **83**, pp. 263–286.
- SANDMEIER, S.R., 2000, Acquisition of bidirectional reflectance factor data with field goniometers. *Remote Sensing of Environment*, **73**, pp. 257–269.
- STANDISH, E.M., NEWHALL, X.X., WILLIAMS, J.G. and YEOMANS, D.K., 1992, Orbital ephemerides of the sun, moon and planets. In *Explanatory Supplement to the Astronomical Almanac*, P.K. Seidelmann (Ed.), pp. 279–374 (Mill Valley, CA: University Books).
- STROPIANA, D., PINNOCK, S., PEREIRA, J.M.C. and GRÉGOIRE, J.M., 2002, Radiometric analysis of SPOT-VEGETATION images for burnt area detection in Northern Australia. *Remote Sensing of Environment*, **82**, pp. 21–37.
- SWAIN, P.H. and DAVIS, S.M., 1978, *Remote Sensing: The Quantitative Approach*, chapter 3 (New York: McGraw-Hill).
- TRIGG, S., 2002, Towards improving the use of remote sensing for monitoring burnt vegetation in African savannahs. PhD thesis, University of Greenwich.
- TRIGG, S. and FLASSE, S., 2000, Characterizing the spectral–temporal response of burned savannah using *in situ* spectroradiometry and infrared thermometry. *International Journal of Remote Sensing*, **21**, pp. 3161–3168.
- TRIGG, S. and FLASSE, S., 2001, An evaluation of different bi-spectral spaces for detecting burned shrub-savannah. *International Journal of Remote Sensing*, **22**, pp. 2641–2647.
- VERSTRATE, M. and PINTY, B., 1996, Designing optimal spectral indexes for remote sensing applications. *IEEE Transactions on Geoscience and Remote Sensing*, **34**, pp. 1254–1265.